Isotropic spin-1 chains with bond alternation: analytic and numerical studies

1995 J. Phys.: Condens. Matter 7 4895

(http://iopscience.iop.org/0953-8984/7/25/014)

J. Phys.: Condens. Matter 7 (1995) 4895–4920. Printed in the UK

Isotropic spin-1 chains with bond alternation: analytic and numerical studies

Keisuke Totsuka†, Yoshihiro Nishiyama, Naomichi Hatano and Masuo Suzuki

Department of Physics, University of Tokyo, 7-3-1 Hongo, Bunkyo-ku, Tokyo 113, Japan

Received 3 January 1995, in final form 23 March 1995

Abstract. Isotropic spin-1 chains with bond alternation are studied. Analytic (both variational and perturbative) results are presented. A phase transition is found to separate the $S = 1$ Haldane phase and the dimer phase. The critical point is numerically determined using the Binder parameter. The universality class is predicted to be given by the level-1 SU(2) Wess–Zumino–Witten model, and this prediction is supported by the present exact diagonalization study. The dimer phase is found to be connected to the '$S = 2$' Haldane phase in a special limit. The change of the excitation spectra and the string order parameter with bond alternation is discussed.

1. Introduction

In 1983, Haldane [1,2] predicted that the Heisenberg chain with integral spins has a disordered ground state above which a finite excitation gap opens, while the half-odd-integral chain has a critical ground state with a gapless excitation. Since the latter seems to be plausible in view of both naive spin-wave theory and the exact solution for $S = 1/2$ [3], much effort was devoted (see, for example, [4]) to understanding the novel massive behaviour of the integer-S chain even after his prediction was confirmed both numerically [5,6] and experimentally [7–9].

One approach may be to understand the spin-$2S$ Heisenberg model as a special limit of the spin-S case. Consider the spin-S Heisenberg chain with bond alternation:

$$\mathcal{H}(J') = \sum_j \boldsymbol{S}_{2j} \cdot \boldsymbol{S}_{2j+1} + J' \sum_i \boldsymbol{S}_{2i-1} \cdot \boldsymbol{S}_{2i}. \tag{1}$$

For convenience, the strength of the exchange interaction of the first term has been set to unity. For $J' = 1$, it reduces to the ordinary Heisenberg antiferromagnet. On the other hand, when we take the limit $J' \to -\infty$, each spin pair of the neighbouring sites $(2i-1, 2i)$ is coupled ferromagnetically, and the model reduces to (within the first-order perturbation theory for the degenerate ground state) the spin-$2S$ Heisenberg chain. Hida [10] developed such an idea for the $S = 1/2$ case and showed that the dimer phase of the $S = 1/2$ chain is smoothly connected to the $S = 1$ Haldane phase without any phase transition (see also [11, 12] for studies in this direction). This indicates that the ($S = 1$) Haldane phase can be interpreted as a special limit of the $S = 1/2$ dimer phase. From this viewpoint the $S = 1$ case of the Hamiltonian (1) would be interesting, since the point $J' = 1$ (no alternation)

† e-mail: TOTSUKA@tkyux.phys.s.u-tokyo.ac.jp

0953-8984/95/254895+26$19.50

belongs to the $S = 1$ Haldane phase, while the limit $J' \to -\infty$ is considered to be in the $S = 2$ Haldane phase. If an essential equivalence between the $S = 1$ dimer phase and the $S = 2$ Haldane phase is confirmed, we can conclude that the $S = 1$ Haldane phase and the $S = 2$ phase are different; there is a phase transition (discussed below in detail) between the two phases.

It may be of interest to study the Hamiltonian (1) from the point of view of the dimerization transition [13, 14]. Using a field-theoretical argument, Affleck and Haldane [15, 16] predicted that second-order transitions occur $2S$ times when we vary J' from $J' = +\infty$ to $J' = 0$. On the other hand, Guo and co-workers [14] discussed the problem by means of a numerical calculation and a physical argument, and concluded that the situation is different for $S \in \mathbb{Z}$ and $S \in \mathbb{Z} + 1/2$ in (1). That is, the transitions occur at non-zero values of J' for integer S, while the ground state is partially or completely dimerized by infinitesimal alternation for half-odd-integer S. Hence we would like to locate precisely the (non-zero) transition point and clarify the nature of the critical point for the smallest integral S.

The present paper is organized as follows. In section 2, we perform a simple variational calculation for the Hamiltonian

$$\mathcal{H} = \sum_i f_\beta(S_{2i} \cdot S_{2i+1}) + J' \sum_j f_\beta(S_{2j-1} \cdot S_{2j}) \tag{2}$$

where the choice of the second-order polynomial $f_\beta(x) = x - \beta x^2$ is generic for isotropic spin-1 chains with a nearest-neighbour interaction. When the bond alternation is absent, exact (and rigorous) results are available for the following four cases: $\beta = -1$ [17, 18], $\beta = -1/3$ [19], $\beta = 1$ [20, 21], and $\beta \to \infty$ [22, 23].

Decreasing the value of J' from one to zero, we expect a phase transition from the $S = 1$ Haldane phase to the dimer phase (provided that $\beta > -1/3$). Using the result of our variational calculation, we obtain a crude estimate of the phase boundary beyond which the string order parameter [24, 25] vanishes. A perturbative estimate of the spectrum near $J' = 0$ is also given.

Section 3 is devoted to a detailed discussion of the Haldane–dimer transition. First, we determine the critical point of the Haldane–dimer transition for the Heisenberg point ($\beta = 0$) numerically by means of exact diagonalization. Owing to the smallness of available system sizes, it is not easy to determine the critical point by the excitation gap. To circumvent this difficulty, we used the finite-size scaling of the Binder parameter. In ordinary cases, the Binder parameter with respect to a certain order measured by a local operator (for example, the ferromagnetic order) is used for order-to-disorder transitions. In our case, on the other hand, such a local order parameter vanishes on both sides of the critical point, and hence the transition is a disorder-to-disorder one in this sense. However, if we use the non-local string order parameter, this method works. The intersection of the Binder parameter for several system sizes yields $J'_c = 0.595 \pm 0.010$. It is also argued that the gap does not close in the region $J' < 0$. This implies that the $S = 1$ dimer phase and the $S = 2$ Haldane phase are smoothly connected.

Then, with combined use of several arguments, we predict that the universality class is the same as that of the level-1 SU(2) Wess–Zumino–Witten (WZW) model. This is confirmed by numerical calculations. Since it is difficult to extract precise values of exponents from numerical data for system sizes up to $L = 16$, we used the excitation spectrum at the critical point to compare with the CFT predictions. Our main results are given in this section.

In section 4, we compute several critical exponents to compare with the analytical prediction. Our numerically estimated values are given as follows: the exponent for the mass gap $\nu = 0.75 \pm 0.05$, the correlation exponents $\eta_{\text{Néel}} = 0.70 \pm 0.10$ and $\eta_{\text{string}} = 0.25 \pm 0.05$.

We numerically study the qualitative change in the spectral property and the string order parameter in section 5. A brief discussion about the difference in the elementary excitation between the critical point and other points is also given.

2. Analytic treatment of the Haldane–dimer transition

In this section, we describe a simple variational treatment of the Haldane–dimer transition and give a qualitative phase diagram. A perturbative estimate of the excitation spectrum near $J' = 0$ is also presented.

First we briefly recapitulate the field-theoretic prediction by Affleck and Haldane [15, 16]. Their argument exploits the large-S mapping to the $O(3)$ non-linear sigma model. Applying the method used in [15] to the Hamiltonian (2), we obtain the $O(3)$ non-linear sigma model with the Π_2-topological term

$$\mathcal{L} = \frac{1}{2g}\partial_\mu \vec{\varphi} \cdot \partial^\mu \vec{\varphi} + \frac{\theta_{\text{top}}}{8\pi}\epsilon^{\mu\nu}\vec{\varphi} \cdot (\partial_\mu \vec{\varphi} \times \partial_\nu \vec{\varphi}) \tag{3}$$

with $g = (1+J')/\sqrt{J'}S$ and $\theta_{\text{top}} = 4\pi S/(1+J')$. If the $O(3)$ non-linear sigma model with $\theta_{\text{top}} = \pi \pmod{2\pi}$ represents a massless theory, we have S massless points in the interval $0 < J' < 1$. Hence in our $S = 1$ case, there is a single second-order transition in that region. Translating the system by one site and replacing J' by $1/J'$, the same argument is also applicable to the case $J' > 1$. However, since the above expression for θ_{top} does not include β, we cannot predict the β dependence of the critical values $\{J'_c\}$.

In order to see the β dependence of J'_c, we perform a simple variational calculation. In constructing a variational wavefunction for our Hamiltonian (2), we have to keep in mind the following two points. (i) The ground state is a singlet state. This can be rigorously proved around the bilinear point ($\beta \approx 0$) [26]. (ii) The ground state smoothly interpolates the valence bond solid (VBS) state [19] ($\beta = -1/3$, $J' > 0$) and the dimer state ($\beta > -1/3$, $J' = 0$). The simplest choice satisfying the above requirement may be

$$|\text{trial}; \Theta\rangle = \cos\Theta \frac{|\text{VBS}\rangle}{||\text{VBS}||} + \sin\Theta \frac{|\text{dimer}\rangle}{||\text{dimer}||}. \tag{4}$$

The above two states $|\text{VBS}\rangle$ and $|\text{dimer}\rangle$ are compactly written as matrix products [27, 28]:

$$|\text{VBS}\rangle = \text{Tr}\, g_1 \otimes g_2 \otimes \cdots \otimes g_L$$

with

$$g_i = \begin{pmatrix} -|0\rangle_i & -\sqrt{2}|1\rangle_i \\ \sqrt{2}|-1\rangle_i & |0\rangle_i \end{pmatrix}$$

and

$$|\text{dimer}\rangle = \text{Tr}\, g_1^{\text{A}} \otimes g_2^{\text{B}} \otimes g_3^{\text{A}} \otimes \cdots \otimes g_{L-1}^{\text{A}} \otimes g_L^{\text{B}}$$

with

$$g_i^{\text{A}} = (|-1\rangle_i, |0\rangle_i, |1\rangle_i) \qquad g_j^{\text{B}} = \text{T}(|1\rangle_j, -|0\rangle_j, |-1\rangle_j).$$

Since the overlap

$$\frac{\langle \text{dimer}|\text{VBS}\rangle}{||\text{dimer}|| \cdot ||\text{VBS}||}$$

decreases exponentially with system size, i.e. $(-1/\sqrt{3})^{L/2}$), this trial state (4) is normalized correctly in the infinite-volume limit. Using the matrix formalism [28], the quantity

$$\epsilon(\Theta) = \lim_{L\nearrow\infty} \frac{1}{L}\langle \text{trial}; \Theta|\mathcal{H}|\text{trial}; \Theta\rangle \tag{5}$$

can be evaluated straightforwardly. The result is given by

$$\epsilon(\Theta) = -\{[\tfrac{1}{3}(1+J')(2+3\beta) - \tfrac{2}{3}\beta J' - 1 - 2\beta]\cos^2\Theta + (\tfrac{2}{3}\beta J' + 1 + 2\beta)\}. \tag{6}$$

Minimization of this quantity yields the variational solution $|\text{trial}; \Theta = 0\rangle$ for $J' > J'_c$ and $|\text{trial}; \Theta = \pi/2\rangle$ for $J' < J'_c$. The critical value gives the transition line

$$J'_c(\beta) = \frac{3\beta+1}{\beta+2} \qquad J'_c(\beta) = \frac{\beta+2}{3\beta+1}. \tag{7}$$

In deriving the second value of J'_c, we have used the symmetry under $J' \to 1/J'$. We show the phase diagram in figure 1. In our calculation, the transition occurs from the perfect VBS phase to the perfect dimer phase. Of course, this is not the true situation. In particular, at the Heisenberg ($\beta = 0$) point, the Haldane–dimer transition occurs at $J' = 0.5$. It is to be compared with the previous estimates of $J'_c \sim 0.6$ (by Singh and Gelfand [29]) and 0.6 (by Kato and Tanaka [30]). Within our simplest approximation, the spontaneous dimerization occurs along the line $J' = 1$, $\beta > 1/2$. It is believed that the end point of the spontaneous-dimerization line is located at the Takhtajan–Babudjian point ($J' = 1$, $\beta = 1$) [31] and hence our analysis underestimates the true value. However, we expect that our phase diagram obtained by the simplest approximation is qualitatively correct.

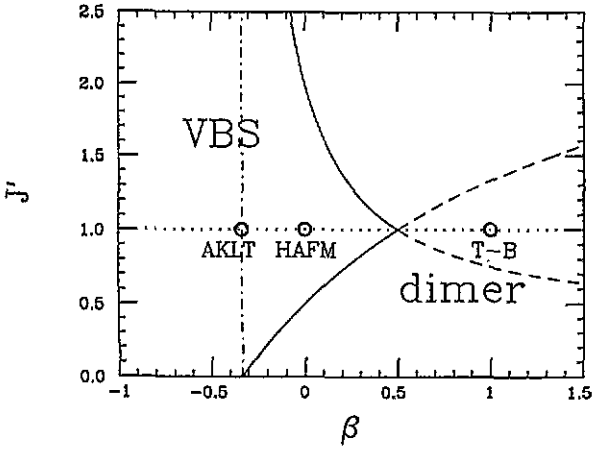

Figure 1. The phase diagram obtained on the basis of the variational wavefunction of section 2. The full curves indicate the phase boundary. The VBS state is the exact ground state on the chain line. Also plotted are (i) the AKLT point, (ii) the $S = 1$ Heisenberg (HAFM) point, and (iii) the Takhtajan–Babujian (TB) point.

To conclude this section, we investigate the Haldane–dimer transition from the viewpoint of the excitation spectrum. Since the Hamiltonian does not allow an exact solution, only restricted pieces of information are available by analytic methods. One of them is the (approximate) excitation spectrum near the dimer point ($J' = 0$, $\beta > -1/3$).

For $J' = 0$, the model is trivial; we readily find that the first excited states are obtained by replacing one of the valence bonds by a triplet bond (i.e. 'crackion' [28, 32]). It has spin-1 and is $N(= L/2)$-fold degenerate positionally. If we turn on the exchange interaction J', the triplet bond made by breaking a singlet valence bond can hop to the neighbouring links with an amplitude proportional to J'. We treat this effect using the degenerate perturbation. The calculation is straightforward and we obtain the following dispersion relation of the triplet ($S = 1$) excitation:

$$\epsilon(k) = (3\beta + 1) - \tfrac{2}{3}J'(\beta + 2)\cos k \tag{8}$$

where the momentum k runs between $-\pi/2a$ and $\pi/2a$. Note that the shape of this spectrum is the same as that of the approximately obtained spectrum of the $S = 1$ VBS model [33] by means of the single-mode approximation. Furthermore, such excitations can be created by the action of a magnon operator $S(k)$ (the Fourier transform of S_i) just as in the VBS case [28, 34].

The shape of $\epsilon(q)$ given by (8) is different qualitatively for $J' > 0$ and $J' < 0$. For $J' > 0$ (the antiferromagnetic region), the excitation gap $(3\beta + 1) - (2/3)J'(\beta + 2)$ exists at $k = 0$. On the other hand, for $J' < 0$ (the ferromagnetic side) it opens at $k = \pi$, and the spectrum is of VBS type. Intuitively, the site-wise short-range AF order (for example, $\ldots, 1, -1, 1, -1, 1, -1, \ldots$) changes into a pair-wise one (for example, $\ldots, 1, 1, -1, -1, 1, 1, -1, -1, \ldots$) at $J' = 0$.

The gap (at $k = 0$) on the AF side decreases as J' increases and we expect that it vanishes at some value of J'. This is the Haldane–dimer transition. If we determine the transition point where the gap vanishes, we obtain

$$J'_c(\beta) = \frac{3}{2}\left(\frac{3\beta + 1}{\beta + 2}\right).$$

However, our perturbative calculation may not be reliable at such a large value as the gap collapses.

3. Determination of the critical point and analysis of the critical point

In this section, we determine precisely the critical point of the Haldane–dimer transition for the system (1), or the $\beta = 0$ case of the generic model (2). In doing this, we made use of the finite-size scaling of the Binder parameter. Then, using these results, we analyse the excitation spectrum for the critical point to compare it with the CFT prediction made below. The exact diagonalization was performed for system sizes up to $L = 16$ using the Lanczos method.

In estimating the critical point, we employ two types of methods. One concerns the finite-size scaling behaviour of the first excitation energy, while the other adopts the Binder parameter defined with respect to the string order.

The critical point is determined as follows. The first-excitation energy obeys the following finite-size scaling relation:

$$\Delta E(L) = \frac{1}{L}Q(L/\xi) \tag{9}$$

where the quantity ξ denotes the correlation length. Since ξ diverges at the critical point, the dimensionless quantity $L\Delta E(L)$ is independent of the system size L. In figure 2, we plot $L\Delta E(L)$ as a function of the parameter J' for various system sizes. Around the region $J' \approx 0.6$, we see that there might be a critical point J'_c and that no further phase transition occurs in the region $J' < 0$ as well as in the region $0 < J' < J'_c$. Thus we conclude that the ground state of the dimer system $J' \approx 0$, and that of the $S = 2$ Heisenberg chain appearing in the limit $J' \to -\infty$ belong to the same unique phase. This is similar to the situation for the $S = 1/2$ case [10] of (1).

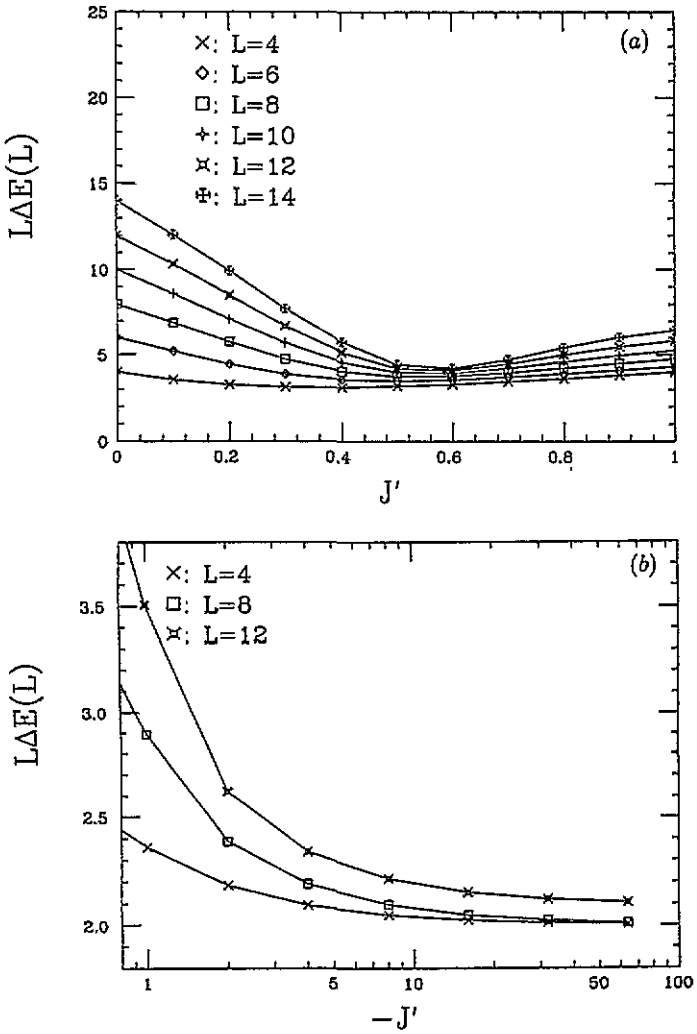

Figure 2. The scaled energy gap, $L\Delta E(L)$, with varying J'. (*a*) $J' > 0$ and (*b*) $J' < 0$.

For a more precise estimate of the critical point J'_c, we introduce the Binder parameter [35–37]

$$U(L, J) = 1 - \frac{\langle O^4 \rangle}{3\langle O^2 \rangle^2}. \tag{10}$$

Here we define the order parameter O in the following form

$$O = \sum_{j=1}^{L} O_j \qquad O_j = \exp\left(i\pi \sum_{k=1}^{j-1} S_k^z\right) S_j^z \tag{11}$$

with respect to the string correlation. It is well known that there exists a long-range string order

$$\lim_{|i-j|\nearrow\infty} \langle O_i O_j \rangle \neq 0$$

at least at the Heisenberg point $J' = 1$. The main idea of our method is as follows. Usually, the Binder parameter is used for transitions that separate the *ordered* phase from the disordered one. On the other hand, in the Haldane–dimer transition, *both* sides of the transition point are disordered in the ordinary sense and hence a naive application of it based on local order parameters does not work well. However, it can be proven [38] that the string order actually vanishes around the dimer line $J' \approx 0$. Assuming that the string order vanishes in the region $J' < J_c'$ as well, the Haldane–dimer transition can be regarded as a kind of order-to-disorder transition with respect to the string order. Thus the Binder parameter is applicable.

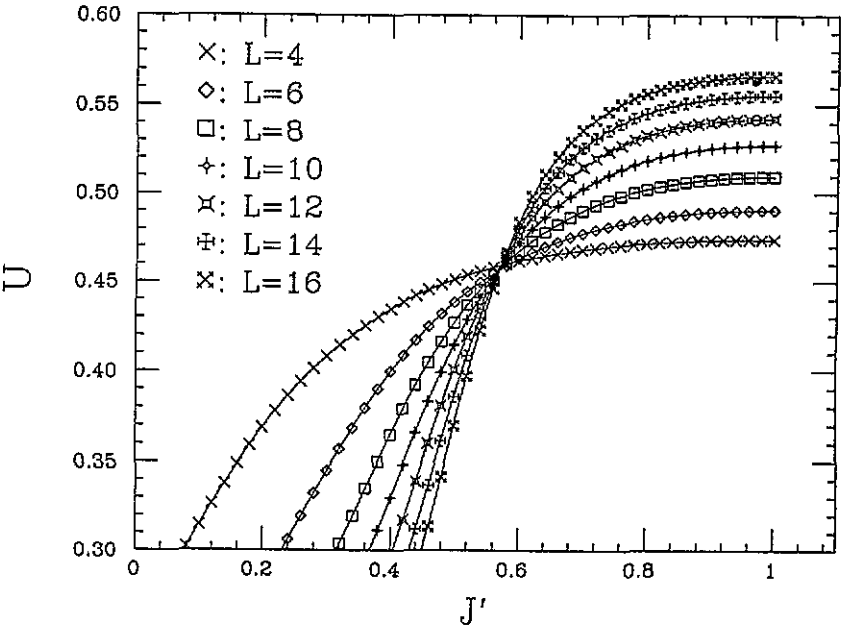

Figure 3. The Binder parameter (10) for $L = 4, 6, \ldots, 16$ with the bond alternation J' varied.

At the critical point, the Binder parameter is invariant under system size L. In the phase where the order parameter O is long-ranged (short-ranged), the Binder parameter $U(L, J)$ increases (decreases) with increasing N. We plot the Binder parameter for various system sizes in figure 3. A co-intersection is found near the point $J' \approx 0.6$. This corresponds to the critical point above observed in figure 3(a). In figure 4 we plot the approximate critical

point $J_c'(L, L+2)$ against the inverse of the system size L. We define the approximate critical point $J_c'(L, L+2)$ by the following relation

$$U\big(L, J_c'(L, L+2)\big) = U\big(L+2, J_c'(L, L+2)\big). \tag{12}$$

From this, we have estimated the extrapolated critical point as

$$J_c' = 0.595 \pm 0.010. \tag{13}$$

This value is consistent with other studies [29, 30]. The fact that the method works well, in its turn, proves the validity of our assumption made above.

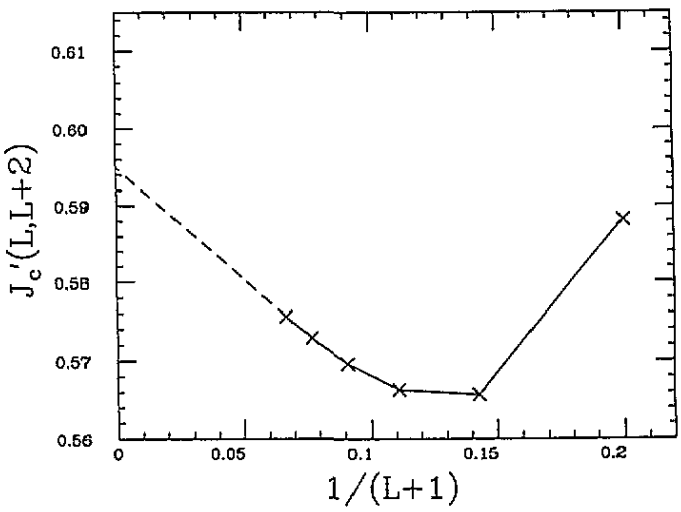

Figure 4. The approximate critical points $J_c'(L, L+2)$ plotted against $1/(L+1)$.

We then proceeded to analyse the excitation spectrum of the model (1) at the critical point $J' = J_c'$. We calculated the excitation energy over the ground state for the system size $L = 16$. The energy levels are plotted against momentum for several values of the z component of the total spin in figure 5(c). Note that the Brillouin zone is reduced by half because of the doubling of the unit cell. In figure 5(c), we can see that the lower edge of the spectrum is almost linear for small values of k. This is one of the features of relativistic massless theories, and hence we can expect that the low-energy behaviour of the model (1) for $J' = J_c'$ is described by the two-dimensional CFT.

There has been some work published concerning the Haldane–dimer transition. The first was that of Affleck and Haldane [15, 16]. They argued that alternating spin-S chains at their critical point can be mapped onto the $O(3)$ NLσM with $\theta_{\text{top}} = \pi$ in the large-S limit. As field-theoretical analyses by several authors [16, 39] suggest that, in the infrared limit, it reduces to the level-1 ($k = 1$) SU(2) WZW model [40, 41] we may expect that the infrared effective theory of the critical point is given by the WZW model. As was seen in section 2, a defect of this argument is that the critical point J_c' is independent of β, in contrast to our variational result (7) and the result of the series expansion [29].

The second paper concerning the Haldane–dimer transition is a numerical calculation of Kato and Tanaka [30]. With combined use of White's method and the finite-size-correction

method, they concluded that the central charge of the Haldane–dimer transition is one. (For the central charge evaluated by the quantum Monte Carlo method, see [72].) Note that the central charge of the $k = 1$ SU(2) WZW model is also equal to one.

Another insight is obtained by mapping our $S = 1$ model (2) onto the 19-vertex-type model with inhomogeneous interactions, which can be viewed as the superposition of the Ising model and the six-vertex model. This is a generalization of the argument developed by den Nijs and Rommelse [24]. According to this argument, the six-vertex degrees of freedom become critical at the Haldane–dimer transition, and hence the central charge is given by unity. Taking into account the SU(2) symmetry, we can expect the universality class to be given by the level-1 SU(2) WZW model.

Let us verify that the massless behaviour observed at $J' = J'_c$ is indeed the same as is expected from the level-1 WZW model. Before describing the details, we briefly summarize the necessary facts about the $k = 1$ SU(2) WZW model. For further details see, for example, [42].

It is well known that the $k = 1$ SU(2) WZW model is realized by a single free boson φ (mathematically, such a realization is known as the Frenkel–Kac construction [43]), which is governed by the following action:

$$S = \int \mathrm{d}^2x \frac{1}{2\pi} \partial_\mu \varphi \partial^\mu \varphi. \tag{14}$$

The two-dimensional spacetime (σ, t) $(0 \leqslant \sigma \leqslant 2\pi)$ is expressed by the light-cone coordinate $x^\pm = t \pm \sigma$. The boson field φ takes its value on a circle of radius R, namely $\varphi \sim \varphi + 2\pi R$. The compactification radius R carries the information of the original (interacting) model. The field φ (and its dual $\tilde{\varphi}$) allows the chiral decomposition

$$\varphi(\sigma, t) = \varphi_{\mathrm{L}}(x^+) + \varphi_{\mathrm{R}}(x^-) \qquad \tilde{\varphi}(\sigma, t) = \varphi_{\mathrm{L}}(x^+) - \varphi_{\mathrm{R}}(x^-)$$

where $\varphi_{\mathrm{L/R}}$ are the chiral bosons defined by the following mode expansions:

$$\varphi_{\mathrm{L}}(x^+) = \tfrac{1}{2} Q + \tfrac{1}{2}(\tfrac{1}{2}\hat{P} + NR)x^+ + \frac{\mathrm{i}}{2} \sum_{n \neq 0} \frac{a_n^{\mathrm{R}}}{n} \mathrm{e}^{-\mathrm{i}nx^+}$$

and $\varphi(x^-)$ is obtained by replacing $x^+ \to x^-$, $N \to -N$, $a_n^{\mathrm{R}} \to a_n^{\mathrm{L}}$. For these operators to satisfy the canonical commutation relations, we impose

$$[Q, \hat{P}] = \mathrm{i} \qquad [a_n^{\mathrm{L/R}}, a_m^{\mathrm{L/R}}] = n\delta_{n+m,0}.$$

Because of the periodicity of φ, the momentum $\hat{P}$ is quantized as M/R. In the following argument, we also use complex coordinates:

$$z = \mathrm{e}^{\mathrm{i}x^+} \qquad \bar{z} = \mathrm{e}^{\mathrm{i}x^-}.$$

Using z and $\bar{z}$ instead of $x^\pm$, the above mode expansion becomes the formal Laurent series.

The so-called vertex operator

$$V_{M,N}(z, \bar{z}) = :\exp\left[2\mathrm{i}\left(\frac{M}{2R} + NR\right)\varphi_{\mathrm{L}}(z) + 2\mathrm{i}\left(\frac{M}{2R} - NR\right)\varphi_{\mathrm{R}}(\bar{z})\right]: \qquad M, N \in \mathbb{Z} \tag{15}$$

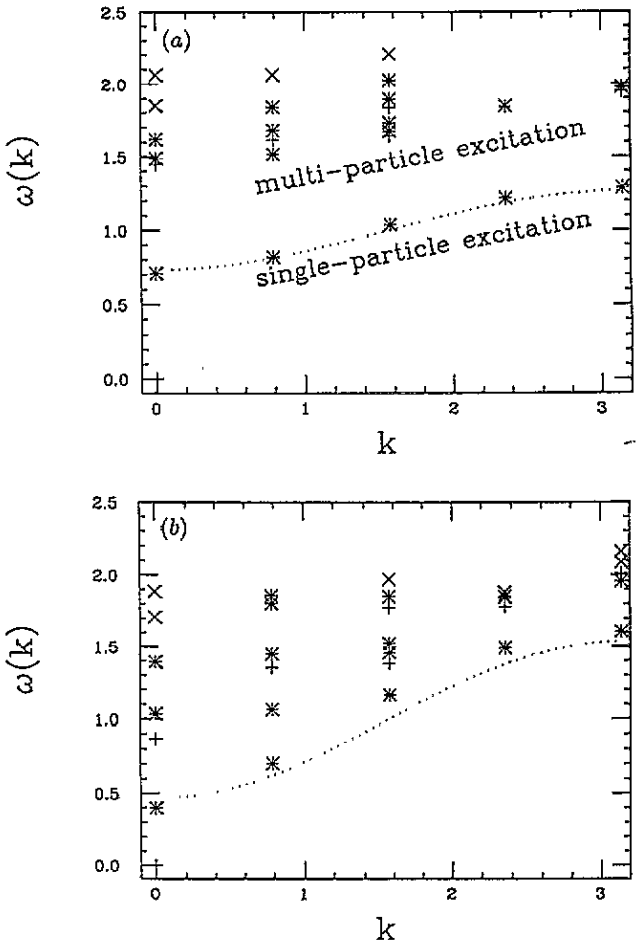

Figure 5. The excitation spectrum for the system size $L = 16$ and the parameter (*a*) $J' = 0.2$, (*b*) $J' = 0.4$, (*c*) $J' = 0.6$ and (*d*) $J' = 0.8$. The symbols +, ×, ◇ and □ stand for levels with quantum numbers $\sum_i S_i^z = 0, 1, 2$ and 3, respectively. The symbols A1–B3 and C are defined in the text (see section 3). The single-magnon ('crackion') branch $\omega(k) = 1 - \frac{4}{3}J'\cos k$ obtained by the perturbation in section 2 is plotted by the dotted curve.

(where $:\cdots:$ denotes normal ordering) create the primary state with the conformal weight [43]

$$\left[\frac{1}{2}\left(\frac{M}{2R} + NR\right)^2, \frac{1}{2}\left(\frac{M}{2R} - NR\right)^2\right]. \tag{16}$$

In our problem, the quantity M (the $U(1)$ charge) can be identified with S^z_{tot}. Note that this type of primary field corresponds to continuously varying critical exponents [44, 45]. At the value $R = 1/\sqrt{2}$, this model realizes the ($\widehat{\text{su}(2)} \times \widehat{\text{su}(2)}$-symmetric) WZW model (see [46] for a more detailed account for the $c = 1$ CFT).

The (finite-size) spectrum expected from the WZW CFT

$$E = \tfrac{1}{2}(M^2 + N^2) + N_{\text{L}} + N_{\text{R}} \qquad P = MN + N_{\text{L}} - N_{\text{R}} \tag{17}$$

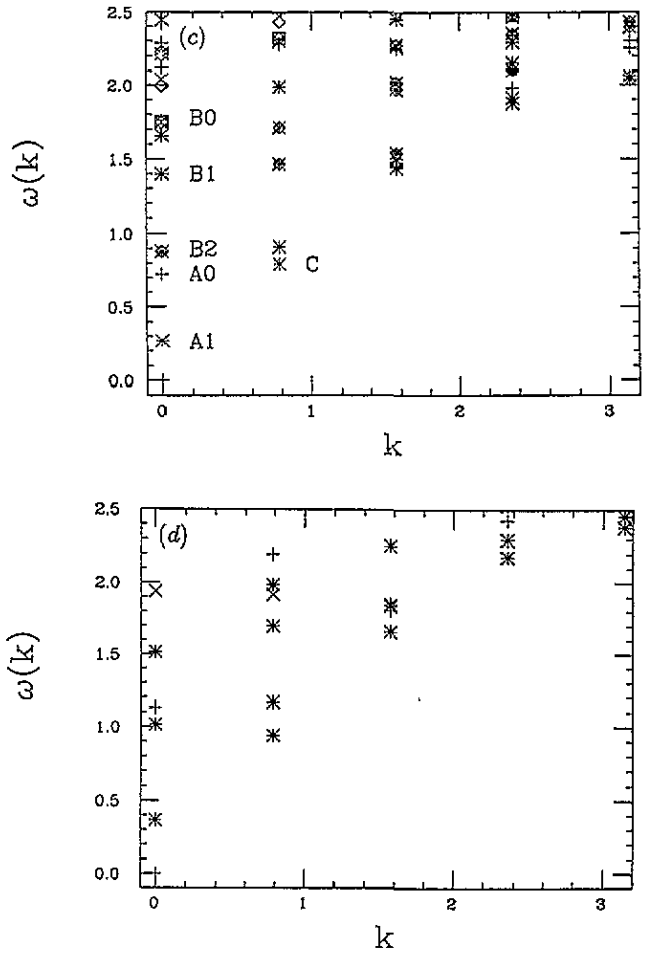

Figure 5. (Continued)

$(M, N, N_L, N_R \in \mathbb{Z})$ is given in figure 6 (where we have chosen the units of E and P as $2\pi v_F/L$ and $2\pi/L$, respectively) together with the eigenvalue of the total spin. In the WZW model, the spins S_L and S_R for left- and right-movers are conserved separately. They are related to the integers M and N by the following equations: $M = S_L^3 + S_R^3$ and $N = S_L^3 - S_R^3$. The degrees of degeneracy $d(E, P)$ are easily obtained by expanding the so-called modular invariant partition function of the WZW model (see, for example, [46]):

$$Z(x, y) = \sum_{E,P} d(E, P) x^E y^P = \sum_{M,N\in\mathbb{Z}} \frac{1}{\prod_{n=1}^{\infty}(1 - x^n y^n)(1 - x^n/y^n)} x^{(M^2+N^2)/2} y^{MN}$$

where

$$x = e^{-2\pi v \mathrm{Im}\tau/L} \qquad y = e^{2\pi i \mathrm{Re}\tau/L}.$$

In-order to know the eigenvalue of S_{tot}, S_L and S_R of each state, we expand another form of the partition function [46]:

$$Z(x, y, z) = \chi_0(xy, z)\chi_0(x/y, z) + \chi_{\frac{1}{2}}(xy, z)\chi_{\frac{1}{2}}(x/y, z)$$

where the quantity χ_j is defined by

$$\chi_j(q,z) = \left(\prod_{n=1}^{\infty}(1-q^n)\right)^{-1} \sum_{n=-\infty}^{\infty} q^{(n+j)^2} z^{n+j}.$$

The coefficient $d(E, P, z)$ of $x^E y^P$ corresponds to the generating function of the multiplicity of the states with a given value of $S^z_{\rm tot}$. The eigenvalues $(S_{\rm tot}, S_{\rm L}, S_{\rm R})$ are also given in figure 7. At first sight, the numerical result (figure 5(*c*)) does not seem to agree with the CFT prediction. However, the discrepancy is resolved as follows. For finite lattice systems, the conformal invariance is only an approximate symmetry, and the systems are regarded as perturbed by irrelevant (and marginally irrelevant) operators [47]. In particular, there is an important marginal operator $J_{\rm L}(z)\cdot J_{\rm R}(\bar{z})$ made up of Kac–Moody currents around the WZW fixed point. It breaks the conformal symmetry of the fixed point and leads to logarithmic corrections for physical quantities.

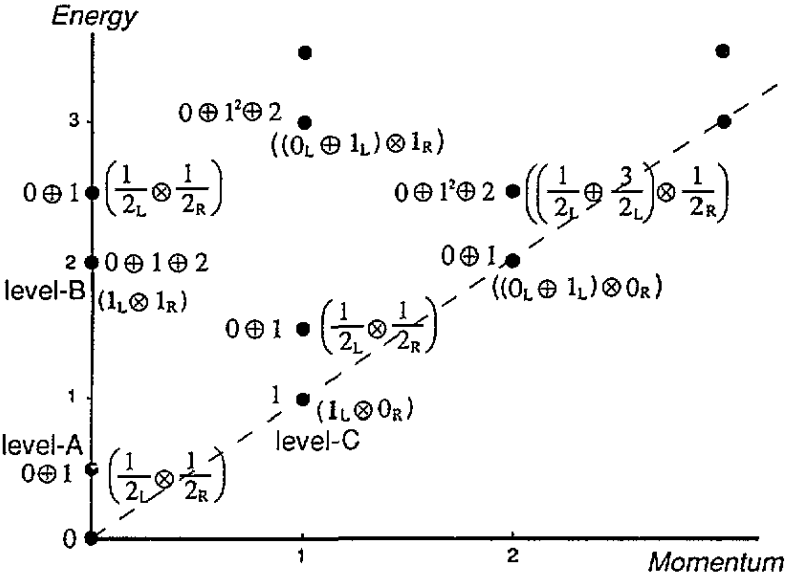

Figure 6. The excitation spectrum expected from the level-1 SU(2) WZW model. The symbols +, ×, ◇ and □ stand for states (k, ω) with quantum numbers $\sum_i S^z_i = 0$, 1, 2 and 3, respectively. The units of the ordinate and abscissa are given by $2\pi v_{\rm F}/L$ ($v_{\rm F} = 1$) and $2\pi/L$. The SU(2) irreducible representations appearing in each state are also shown. The eigenvalues of $S^{\rm tot}_{\rm L}$ and $S^{\rm tot}_{\rm R}$ are shown in parentheses. The three levels used in section 3 are also indicated.

In order to examine whether the numerical spectrum coincides with that of the WZW model, we focus on six energy levels (A0, A1), (B0, B1, B2) and C in figure 5(*c*). The numbers 0, 1 and 2 stand for the eigenvalues of $S_{\rm tot}$. From the relative positions, the spin eigenvalues $S_{\rm tot}$, and the degrees of degeneracy of these levels, we guessed that they correspond to three levels A, B and C in figure 6. If the infinite Kac–Moody symmetry is unbroken, the levels (A0, A1) and (B0, B1, B2) have to group together into two degenerate levels A and B, respectively. Assuming that this splitting of levels is caused by the above marginal operator, the energy levels including the logarithmic correction are given by the

following formula [48]

$$E_i(L) = \frac{2\pi v_F}{L}\left(x_i - \frac{4\pi g(L) S_L^{tot} \cdot S_R^{tot}}{\sqrt{3}}\right) \tag{18}$$

where the quantity $g(L)$ denotes the effective coupling constant for the marginal operator at the length scale L. For large enough L, we can replace $g(L)$ by its asymptotic form $\sqrt{3}/4\pi \ln L$ in the above formula. Therefore, we can eliminate the leading-logarithmic correction by taking weighted averages of the levels [48, 49].

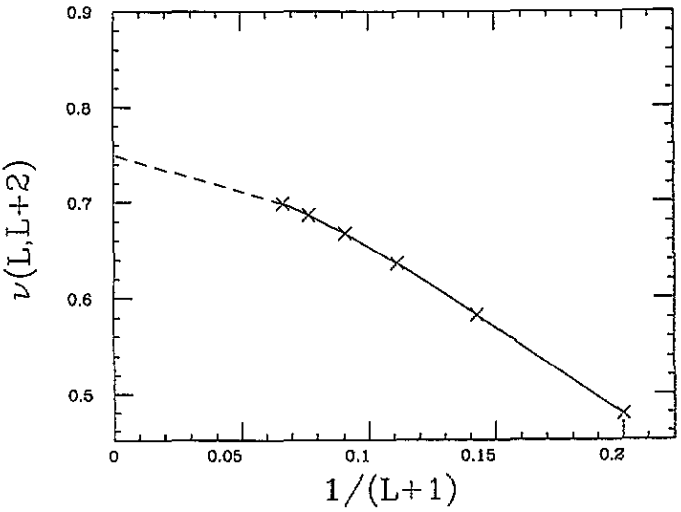

Figure 7. The approximate critical exponents $\nu(L, L+2)$ plotted against $1/(L+1)$.

For the energy $E_A(L)$ of the level A, we take the average

$$E_A(L) = \tfrac{1}{4}E_{A0}(L) + \tfrac{3}{4}E_{A1}(L).$$

There are three ways to take the weighted average for the energy E_B of the level B:

$$\begin{aligned} E_B^1(L) &= 1/2E_{B1}(L) + 1/2E_{B2}(L) \\ E_B^2(L) &= 1/3E_{B0}(L) + 2/3E_{B2}(L) \\ E_B^3(L) &= 2E_{B1}(L) - E_{B0}(L). \end{aligned} \tag{19}$$

For $L = 12, 14, 16$, we verified that the values obtained in these three ways are close to each other. Hence, we can expect that the leading-logarithmic corrections are eliminated in this method. Moreover, this would support our prediction, since it is unlikely that the finite-size splittings are eliminated by this method for other CFT than the SU(2) WZW model. However, in order to preserve the precision, we adopt $E_B^1(L)$, which is obtained from the lowest two levels, B1 and B2, in the following analysis. The residual splitting may be explained by including corrections due to irrelevant operators and the higher-order logarithms like $1/(\ln L)^3$.

We begin with the 'Fermi velocity'. To estimate it, we adopt the following procedure. First, we note that the logarithmic correction in (18) vanishes for the energy level C (provided that the spectrum indeed corresponds to the WZW model), since $S_L^{tot} \cdot S_R^{tot}$ vanishes for this level (see figure 6). Therefore the slope of the segment joining the ground state and the state C gives the desired quantity. From the data for $L = 12, 14, 16$, we extrapolate the quantity $v_F(L) = \frac{L}{2\pi} E_c(L)$ by a second-order polynomial in $1/L$ to obtain

$$v_F = 1.91. \tag{20}$$

This is close to the value obtained in [72] (after multiplying the factor 1.25 of the Hamiltonian) using the quantum Monte Carlo method, while the discrepancy between the density-matrix renormalization group result [30] and ours is rather large.

Using the numerically evaluated Fermi velocity v_F, the scaling dimensions corresponding to levels A and B are estimated by extrapolating the following quantities:

$$x_A(L) = \frac{L}{2\pi v_F} E_A(L) \qquad x_B(L) = \frac{L}{2\pi v_F} E_B(L).$$

The results are given by

$$x_A = 0.51 \qquad x_B = 1.94. \tag{21}$$

These are to be compared with 0.5 (the conformal dimensions of the fundamental field g of the WZW model) and 2 (the scaling dimensions of a Kac–Moody descendant field $J^{\alpha}_{L,-1} J^{\beta}_{R,-1} \mathbf{1}$ at level-2).

We also estimated the central charge from the ground-state-energy data for $L = 10, 12, 14, 16$. Following the standard method [50], we obtained $\frac{1}{6}\pi v_F c = 1.107$, which means $c = 1.10$. Note that the $k = 1$ WZW model has a central charge of unity. Furthermore, this is close to the result of the previous study $c = 1.0 \pm 0.15$ [30].

The agreement is good for the smallness of the system size. That is, we obtained appropriate values of the scaling dimensions and the central charge simply by assuming a few qualitative facts expected from the WZW model, the relative positions of the levels and the form of the logarithmic corrections (18). Thus the spectrum obtained at $J' = J'_c$ is consistent with that predicted on the basis of the $k = 1$ WZW model. The present result does not agree with the prediction of [29] that the critical theory will be the $k = 2$ WZW model.

4. Calculation of several critical exponents

In this section, we report our estimates of the critical exponents ν, $\eta_{\text{Néel}}$ and η_{string}. They are defined by the following relations:

$$m \sim \left(\frac{|J' - J'_c|}{J'_c} \right)^{\nu} \tag{22}$$

$$\langle S^z_i S^z_{i+r} \rangle \sim (-1)^r r^{-\eta_{\text{Néel}}} \qquad \left\langle S^z_i \exp\left(i\pi \sum_{k=i}^{i+r-1} S^z_k \right) S^z_{i+r} \right\rangle \sim r^{-\eta_{\text{string}}} \tag{23}$$

where the quantity m in the first equation denotes the excitation gap.

Before describing the numerical results, we predict these exponents using the level-1 WZW model. We begin by constructing the continuum expression of the string operator. First we have to keep in mind that the invariance of the Hamiltonian (1) under translation by one site is already broken at the critical point. Hence the usual expression [16, 48]

$$S_i \sim J_L + J_R + \text{constant}(-1)^i \operatorname{Tr} g\sigma$$

(where the 2×2-matrix g and σ denote the WZW fundamental field and the Pauli matrices, respectively) cannot be used. Taking into account the doubling of the unit cell, continuum fields have to be defined on two-site cells. Thus we take the spin-density operator as

$$s^{\pm}(\sigma, t) = \frac{S^{\pm}_{2i} + S^{\pm}_{2i+1}}{2a} \sim :\mathrm{e}^{\pm \mathrm{i}2\sqrt{2}\varphi_L(x^+)}: + :\mathrm{e}^{\pm \mathrm{i}2\sqrt{2}\varphi_R(x^-)}: \tag{24}$$

and

$$s^3(\sigma, t) = \frac{S^z_{2i} + S^z_{2i+1}}{2a} \approx \frac{1}{\sqrt{2}\pi}\partial_t \varphi(\sigma, t) = \frac{1}{\sqrt{2}\pi}\partial_\sigma \tilde{\varphi}(\sigma, t). \tag{25}$$

Of course, there might be operators with lower scaling dimensions (i.e. more relevant in the long-distance behaviour) such as $\operatorname{Tr} g\sigma$ whose scaling dimension is 1/2. However, if we note the fact that the spatial integral of the spin density s gives S_{tot} (which preserves the ground-state energy), the possibility of this kind of operator is excluded; in the usual antiferromagnets, there is a quickly varying factor $(-1)^x$ before $\operatorname{Tr} g\sigma$, and hence it does not contribute to S_{tot}. Replacing the summation $\sum_{k=1}^{j}$ by the integration $\int_0^\sigma \mathrm{d}\sigma$ and using the operator-product expansion (OPE), we obtain the desired result:

$$\prod_{k=1}^{j-1} \exp[\mathrm{i}\theta(S^z_{2k} + S^z_{2k+1})](S^z_{2j} + S^z_{2j+1}) \sim :\exp\left[\mathrm{i}\frac{1}{\sqrt{2}}\left(\frac{\theta}{\pi}\right)\tilde{\varphi}(\sigma, t)\right]:. \tag{26}$$

This corresponds to the vertex operator $V_{M=0,N=\theta/2\pi}$, which plays the role of a twist operator† [51] and is missing from the operator content of periodic systems [45, 52]. When $\theta = \pi$ (the ordinary string 1-point function), our result is consistent with the conclusion of Alcaraz and Hatsugai [53]. From the above expression, we readily conclude that the scaling dimensions of this operator and the correlation exponent are given by

$$x_{\text{string}} = \frac{1}{8}\left(\frac{\theta}{\pi}\right)^2 \qquad \eta_{\text{string}} = \frac{1}{4}\left(\frac{\theta}{\pi}\right)^2 \tag{27}$$

respectively.

Another quantity of physical interest may be the form of the string 1-point function and the mass gap in the vicinity of the critical point. To calculate it, we have to know by which operator the system is driven away from the (WZW) critical point. We look for such an operator $\mathcal{O}$ that satisfies the condition of SU(2) invariance i.e. $[S_{tot}, \mathcal{O}] = 0$. It is important to note that, owing to the broken translational invariance, we cannot discard the possibility of a operator $\operatorname{Tr} g$; it is excluded in translationally invariant systems for the reason that it is odd under the discrete symmetry $g \to -g$ [16]. Taking into account that the operator $\operatorname{Tr} g$

† When $\theta = \pi$, it changes the boundary condition for $S^{\pm}$ to antiperiodic one.

is the only relevant operator that satisfies the above condition, we may identify the leading contribution to the perturbing fields with $\mathrm{Tr}\, g$.

The operator $\mathrm{Tr}\, g$ has the scaling dimension 1/2 [41]. Hence a naive expression of the mass gap is given by $m(\lambda) = \lambda^{2/3}$ [13] (where the coupling constant λ is defined by $|J' - J'_c|/J'_c$). However, as is well known [16, 54], an important marginal operator $J_L \cdot J_R$ exists around the WZW fixed point, which yields logarithmic corrections to the scaling behaviour [48, 55, 56]. Using the formula of [48], the mass gap with the logarithmic correction included is predicted to behave as

$$m(\lambda) \sim \frac{\lambda^{2/3}}{|\ln \lambda|^{1/2}}. \tag{28}$$

Combining this with the scaling argument, we obtain the string order parameter as

$$\mathcal{O}_{\mathrm{string}}(\theta) \sim \frac{\lambda^{(\theta/\pi)^2/6}}{|\ln \lambda|^{(\theta/\pi)^2/8}}. \tag{29}$$

This implies that the string order parameter $\mathcal{O}_{\mathrm{string}}$ tends to zero when $J' \to J'_c + 0$. The long-distance limit of the string correlation function G_{string} can also be calculated as

$$G_{\mathrm{string}}(r) \sim \frac{1}{r^{(\theta/\pi)^2/4}[\ln r]^{-(\theta/\pi)^2/8}}. \tag{30}$$

See appendix A for calculational detail.

We now proceed to a numerical calculation. We use the Lanzcos method, as in section 4. The critical exponent ν is estimated as follows. According to the finite-size scaling, the Binder parameter U may be scaled as

$$U(L, J) = \widetilde{U}(L/\xi) = \widetilde{U}\left[L\left(\frac{|J' - J'_c|}{J'_c}\right)^{\nu}\right]. \tag{31}$$

Hence, we obtain the approximate exponent $\nu(L, L+2)$ as

$$\nu(L, L+2) = \ln[(L+2)/L]\left(\ln \frac{U'\big(L+2, J_c(L, L+2)\big)}{U'\big(L, J_c(L, L+2)\big)}\right)^{-1} \tag{32}$$

where

$$U'(L, J) = \left(\frac{\partial U(L, J)}{\partial J}\right)_L. \tag{33}$$

We plot the exponent $\nu(L, L+2)$ against the inverse of the system size in figure 7. We extrapolate the exponent ν as $\nu = 0.75 \pm 0.05$. The agreement with the predicted value 2/3 (see(28)) is not so good. However, there is no relevant scaling field that leads to $\nu \approx 0.75$ in the WZW model, and this discrepancy should be attributed to the finite-size effect and the logarithmic dependence of ν.

The critical exponent $\eta_{\mathrm{Néel}}$ and η_{string} are estimated on the basis of the following relations, which are valid at the critical point:

$$\langle O^2_{\mathrm{Néel}} \rangle \propto L^{-\eta_{\mathrm{Néel}}} \tag{34}$$

$$\langle O^2_{\mathrm{string}} \rangle \propto L^{-\eta_{\mathrm{string}}} \tag{35}$$

where

$$O_{\text{Néel}}(L) = \frac{1}{L}\sum_{j=1}^{L}(-1)^j S_j^z \tag{36}$$

and

$$O_{\text{string}}(L) = \frac{1}{L}\sum_{j=1}^{L} O_j. \tag{37}$$

Therefore, the approximate exponents are given by

$$\eta_\alpha(L, L+2) = \frac{\ln\langle O_\alpha^2(L+2)\rangle - \ln\langle O_\alpha^2(L)\rangle}{\ln(L+2) - \ln L} \tag{38}$$

where O_α denotes $O_{\text{Néel}}$ or O_{string}. The values of (38) are plotted against the inverse of the system size in figures 8 and 9, respectively. Using two points corresponding to the largest two values of L, we can extrapolate the value as

$$\eta_{\text{Néel}} = 0.70 \pm 0.10 \qquad \eta_{\text{string}} = 0.25 \pm 0.05. \tag{39}$$

The estimate of η_{string} depends on the evaluation of J_c'. We have assumed J_c' to obtain the above value. These estimates of the exponent η_{string} are consistent with that of the field-theoretical prediction $\eta_{\text{string}} = 1/4$. From the above result, it seems that the logarithmic dependence of the string correlation function does not appear. This is probably because $(\ln r)^{-1/8}$ is a slowly varying function of r, while the present system size is limited to $L \lesssim 16$.

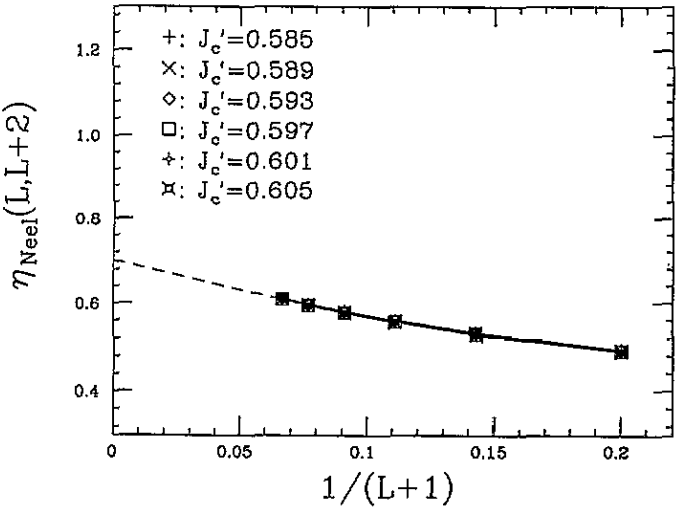

Figure 8. The approximate critical exponents $\eta_{\text{Néel}}(L, L+2)$ against $1/(L+1)$.

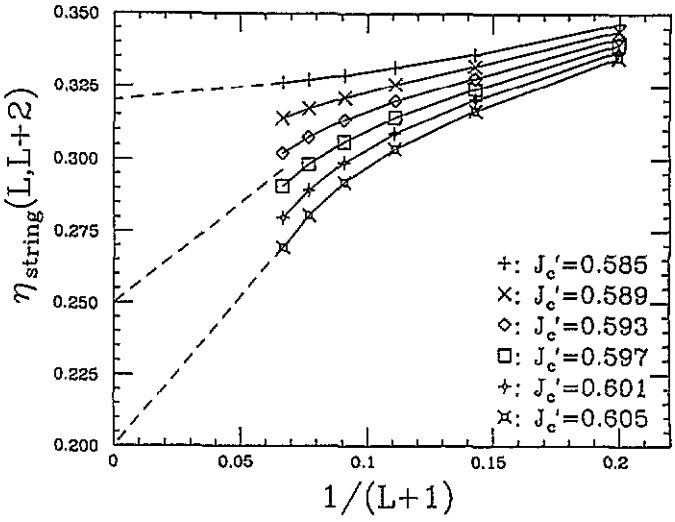

Figure 9. The approximate critical exponents $\eta_{\text{string}}(L, L+2)$ against $1/(L+1)$.

The exponent $\eta_{\text{Néel}} \approx 0.7$ differs from the value of unity expected from the $S = 1/2$ Heisenberg chain [57]. However, the staggered correlation function $G_{\text{stag}}(r) = \langle(-1)^r S_0^z S_r^z\rangle$ is expected to have a logarithmic correction $(\ln r)^{1/2}$ (see appendix A). This factor is not negligible when deriving the approximate exponents by (38). We plotted $rG_{\text{stag}}(r)$ against the distance between the two points and found that it is a slowly increasing function of r. If we regard this behaviour as a consequence of the factor $(\ln r)^{1/2}$, our prediction does not contradict the numerical estimates.

We make the following conclusions. First, we have verified that the string operator O_j is expressed as the vertex operator $V_{M=0,N=1/2}$ (which corresponds to the case $\theta = \pi$ in (26) in the continuum limit. This fact is assumed *ad hoc* in the previous study [53]. Second, the criticality is found to be characterized by the level-1 SU(2) WZW model whose central charge is equal to one, or equivalently, the free boson model (14) with $R = 1/\sqrt{2}$. Our result that the central charge is given by $c = 1$ is consistent with the numerical studies by Kato and Tanaka [30], and Yamamoto [72].

5. The low-lying excitation and the string order parameters

In this section, we investigate the excitation spectrum for various values of the alternation J'. The spectrum is discussed in conjunction with the CFT prediction and the perturbative result described in sections 2 and 3. Hida [58] investigated the spectrum of the model for the case $S = \frac{1}{2}$, the spectra of the model (1) with $S = 1/2$. The peculiar point of the present system is that the transition occurs away from the point $J' = 1$.

First, we show the dispersion relation for $J' = 0.2$, 0.4, 0.6 and 0.8, (the antiferromagnetic side), in figure 5. We have chosen the unit of momentum to be $2\pi/16$. Note that the doubling of the unit cell reduces the size of the Brillouin zone by half ($L_{\text{eff}} = L/2 = 8$). Correspondingly, the gap opens not at $k = \pi$ but at $k = 0$. The spectrum for $J' = 0.2(\approx 0)$ shows that the $S = 1$ single-particle branch is well approximated by the formula (8) derived from the first-order perturbation in J'. Hence, we may expect that the

elementary excitation around $J' = 0$ is created by exciting a singlet bond to a triplet one; see section 2. In other words, the excitation is an $S = 1$ magnon rather than a pair of $S = 1/2$ spinons [20, 59] of the integrable Heisenberg chain. The gap decreases as J' increases and it closes at $J' = J'_c$. At this value, the isolated $S = 1$ single-particle branch mentioned above is absorbed in the continuum of the multiparticle states. Then the degenerate $S = 0$ and $S = 1$ excitations, which actually split in a finite system owing to the logarithmic corrections, at $k = 0$ consist of two massless $S = 1/2$ spinons; a singlet combination of them gives the $S = 0$ excited state and triplet combinations give the $S = 1$ states. This can be understood by the fact that the long-range resonating valence-bond (RVB) state, whose excitation is the spinon [60], would be realized at $J' = J'_c$. Furthermore, the dispersion at the parameter $J' = 0.6 \approx J'_c$ shows characteristics of the massless model, namely the linear dispersion around $k = 0$ and the conformal tower [47]. We have already discussed this spectrum in detail in section 3.

For $J' > J'_c$, the gap Δ_H between the singlet ground state ($k = 0$) and the triplet excited state opens at $k = 0$ and is an increasing function of J'. The $S = 1$ single magnon branch emerges again and seems to persist for $J' = 1$.

Finally, we concentrate on the region $J' < 0$, i.e. the ferromagnetic side. As was explained in section 4, there is no phase transition in the region $J' < 0$; the dimer phase $J' \approx 0$ and the $S = 2$ Haldane phase $J' \to -\infty$ can be viewed as two special limits of the same unique phase. We depict the excitation spectrum for $J = -0.1$, -0.5 and -1 in figure 10. The spectrum for $J' = -0.1$ shows that the excitation is again well approximated by the formula (8) with a negative value of J', as in the above case $J' = 0.2$; the excitation is identified with an $S = 1$ massive magnon. The formula (8) also tells us that the first exited state is located at $k = \pi$ with a excitation gap Δ_H; note that it exists at $k = 0$ in the case $J' > 0$. The other figures for $J' = -0.5$ and -1 are consistent with our conclusion that no phase transition occurs for $J' < J'_c$. Therefore, the elementary excitation of the $S = 2$ Haldane system, which appears as a special limit of our $S = 1$ model, may be the same as that of the $S = 1$ dimer system at $J' = 0$, or the excitation is given by the $S = 1$ massive magnon. This is consistent with Haldane's original argument [1].

For J' smaller than -0.23, the single-magnon branch seems to be absorbed in the multiparticle continuum. This situation is similar to what is well known in the ordinary $S = 1$ Heisenberg chain [61–63]. The estimate $J' = -0.23$ is close to the value -0.25 predicted by the perturbative formula (8). Probably because of the finite-size effect, the lower edge of the multiparticle continuum at $k = 0$ is slightly larger than twice the gap Δ_H at $k = \pi$. Assuming that main features of the spectrum for $J' < 0$ persist even in the limit $J' \to \infty$, we can expect that the $S = 1$ Haldane system and the $S = 2$ system are essentially the same, at least with respect to the spectral property.

Next, we discuss the Haldane–dimer transition in conjunction with the string order parameter. The string order parameter [24, 25] defined by

$$\mathcal{O}^{(\mathrm{I})}_{\mathrm{string}}(\theta) = \lim_{|i-j|\nearrow\infty} \left\langle S^z_i \exp\left(\mathrm{i}\pi \sum_{k=i}^{j-1} S^z_k\right) S^z_j \right\rangle \tag{40}$$

has proved to be useful in detecting the Haldane phase in $S = 1$ chains and has been extensively studied both analytically and numerically [38, 64–67]. Hence it is interesting to investigate how it changes at the Haldane–dimer transition. In the following, we also adopt a modified definition of the string order parameter:

$$\mathcal{O}^{(\mathrm{II})}_{\mathrm{string}}(\theta) = \lim_{|i-j|\nearrow\infty} \left\langle (S^z_{2i-1} + S^z_{2i}) \exp\left(\mathrm{i}\theta \sum_{k=2i-1}^{2j-2} S^z_k\right) (S^z_{2j-1} + S^z_{2j}) \right\rangle. \tag{41}$$

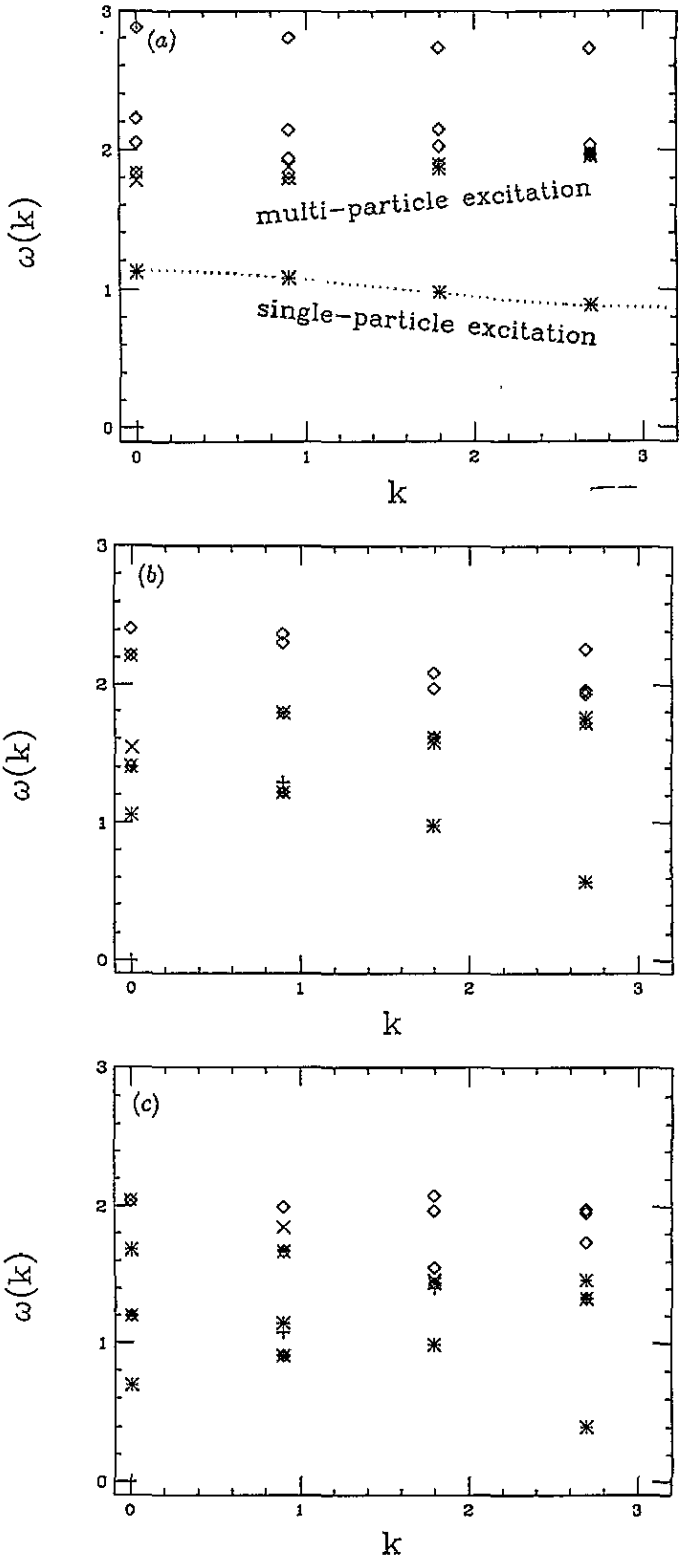

Figure 10. The excitation spectrum for system size $L = 14$ and parameters (*a*) $J' = -0.1$, (*b*) -0.5 and (*c*) -1. The symbols $+$, $\times$ and $\diamond$ stand for levels with quantum numbers $\sum_i S_i^z = 0, 1$ and 2, respectively. The dotted line denotes the single-magnon branch $\omega(k) = 1 - \frac{4}{3}J' \cos k$.

Following Oshikawa [64] and Hida [68], we have adopted a generalized version of the string order parameter obtained by choosing a general angle θ instead of π. As was discussed in [64] and [28], $\mathcal{O}_{\text{string}}(\theta)$ may give some clues to characterizing the phases despite lack of a complete justification of its relevance. In the ferromagnetic limit ($J' \to -\infty$), it reduces to the string order parameter for spin-2S variables [10]. We can compute the quantity $\mathcal{O}_{\text{string}}(\theta)$ using the matrix formalism [28, 69] for the two phases (the $S = 1$ VBS and the dimer) on the both sides of the Haldane–dimer line. The result is given as follows:

$$\mathcal{O}^{(\text{II})}_{\text{string}}(\theta) = \begin{cases} \frac{16}{81}\sin^2\frac{1}{2}\theta & S = 1 \text{ VBS state} \\ \frac{4}{9}\sin^2\theta & S = 1 \text{ dimer state.} \end{cases} \tag{42}$$

It is important to note that their θ dependence is quite different. That is, the string order parameter for $\theta = \pi$ is non-vanishing for the VBS phase, while it is zero in the dimer phase. Moreover, the θ dependence of $\mathcal{O}_{\text{string}}(\theta)$ in the $S = 1$ dimer phase (namely, the double-peak structure) is the same for the one evaluated for the $S = 2$ VBS state. (This can be generalized to higher-S cases, where the same θ dependence is obtained both for the spin-2S VBS state and for the spin-S dimer state.) Of course, the above calculation is based on the variational solution obtained in section 2 and the functional form of $\mathcal{O}_{\text{string}}(\theta)$ does not change in each phase. This is somewhat unrealistic. However, assuming that the global structure of $\mathcal{O}_{\text{string}}(\theta)$ is invariant in each phase of the true (not variational) solution, we can conclude that a drastic change in the θ dependence of the string order parameter does occur at the Haldane–dimer transition. For $J' < J'_c$, $\mathcal{O}_{\text{string}}(\theta)$ becomes to show qualitatively the behaviour in the $S = 2$ VBS state; there are two nodes at $\theta = 0, \pi$ and two peaks are located at $\theta = \pi/2, 3\pi/2$. We may regard these results as a strong support for the correctness of the viewpoint that the spin-S Haldane phase is essentially the same as the spin-$S/2$ dimer phase [10].

We now show the numerical result of two types of the general θ string order parameter, (I) and (II), for system size $L = 12$. For (I):

$$\mathcal{O}_{\text{string}}(\theta, L/2) = \left\langle S^z_1 \exp\left(\mathrm{i}\theta \sum_{k=1}^{L/2} S^z_k\right) S^z_{L/2+1} \right\rangle \tag{43}$$

and for (II):

$$\mathcal{O}_{\text{string}}(\theta, L/2) = \left\langle (S^z_1 + S^z_2) \exp\left(\mathrm{i}\theta \sum_{k=1}^{L/2} S^z_k\right) (S^z_{L/2+1} + S^z_{L/2+2}) \right\rangle. \tag{44}$$

The difference between them for the $S = 1/2$ case is discussed in [70]. They are plotted in figures 11(a) and 11(b), respectively, for $J = -10$, 0.1, 0.6 and 1. We have not yet succeeded in finding the best order parameter. Nevertheless, we may expect that the generalized string order parameter $\mathcal{O}_{\text{string}}(\theta)$ characterizes the nature of the phases in some aspects. The plots behave differently in the two phases $J' < J'_c$ and $J' > J'_c$. In the former, the curve has a single maximum at $\theta = \pi$, while in the latter the maxima are located near $\theta = \frac{\pi}{2}$ and $\theta = \frac{3\pi}{2}$. That is, the qualitative feature of the string correlator changes drastically. This agrees with the prediction based on a simple variational calculation.

The importance of the number of nodes of the string correlator in characterizing the Haldane phases was first pointed out by Oshikawa [64]. In this sense, the drastic change observed above reflects the qualitative difference between the two phases. The remarkable point is that we can also observe the equivalence between the $S = 2$ Haldane phase ($J' = -\infty$) and the trivial dimer phase ($J' \approx 0$) from the point of view of the string correlation function.

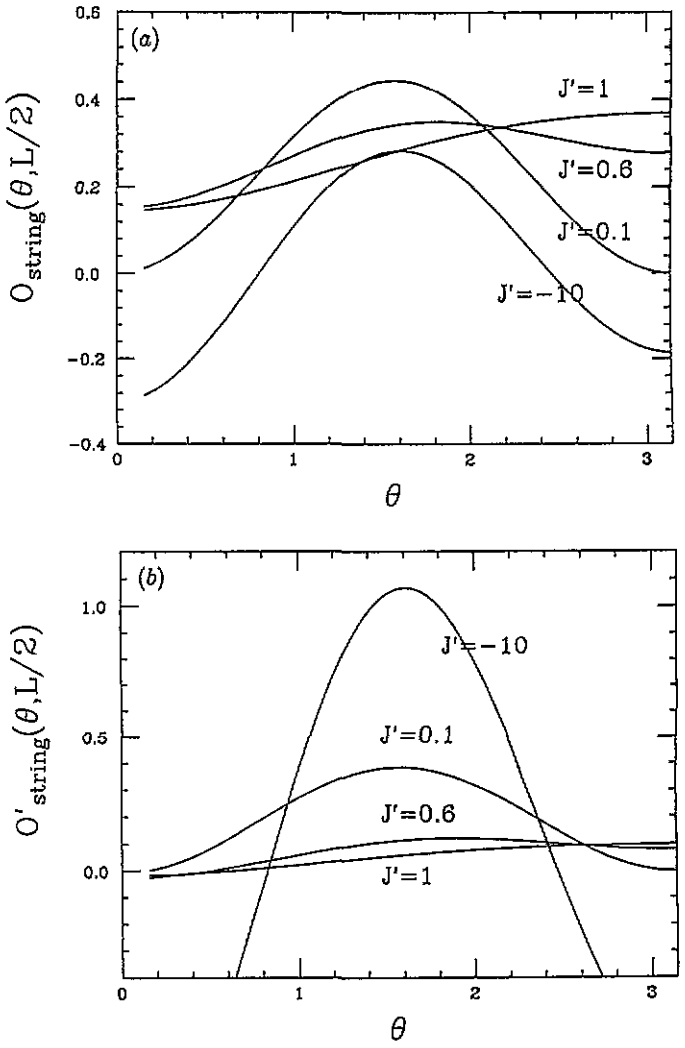

Figure 11. The generalized string correlations, $\mathcal{O}_{\text{string}}(\theta, L/2)$ (*a*) and $\mathcal{O}'_{\text{string}}(\theta, L/2)$ (*b*), plotted against θ for the parameters $J' = -10, 0.1, 0.6$, and 1.

6. Summary and discussions

In the present paper, we have studied the $S = 1$ isotropic spin chain with bond alternation (2), both analytically and numerically. With use of a simple variational wavefunction, we have reproduced the phase diagram for the model (2), which is qualitatively correct. Based on this argument, we have predicted that the qualitative change in the string correlation occurs at the Haldane–dimer transition. We also studied the model (1) for the Heisenberg point $\beta = 0$ numerically and determined the transition point precisely with the combined use of finite-size scaling and the Binder parameter defined for the non-local order parameter. Our method yields a more precise determination of J'_c than do other methods (for example, the direct observation of the gap), despite the smallness of the system size. The fact that our method has worked well implies that the $\theta = \pi$ string order parameter in the infinite-volume

limit actually vanishes for $J' < J'_c$.

The observation of the excitation gap tells us that the phase transition occurs only once in the region $-\infty < J' < 1$ and furthermore that the rather trivial dimer phase ($J' \approx 0$) is smoothly connected to the non-trivial $S = 2$ Haldane phase ($J' \to -\infty$). A similar situation has been observed for the $S = 1/2$ alternating chain. We have thus established the equivalence between the dimer phase and the Haldane phase for $S = 1(\leftarrow 1/2)$ and $S = 2(\leftarrow 1)$, namely both for S odd and for S even. From our viewpoint, the vanishing of the $\theta = \pi$ string order parameter for $S =$ even [64] corresponds to the fact that it vanishes for the $S = 1$ dimer phase. Note that it is impossible to regard chains with half-odd integer S as a limit of a certain dimer system. This is in great contrast to the integer-S chains.

We have predicted that the phase transition that separates the $S = 1$ Haldane phase and the dimer phase is described by the $k = 1$ SU(2) WZW model; this prediction is consistent with the previous field-theoretical [16] and numerical [30] studies. The prediction for several exponents was also given. Although there are severe logarithmic corrections for correlation functions and so on, the numerical estimates do not contradict our prediction.

A close examination of the spectrum of the model (1) showed that the elementary excitation is given by the massive triplet magnon, except at the critical point J'_c. This is consistent with Haldane's conjecture.

At the critical point, the spectrum shows the characteristics of the relativistic massless theory at low energies. We have confirmed that our spectrum does not contradict the CFT prediction of section 3. It is well known [60] that the spinon is a physical excitation in the long-range RVB picture and that the $k = 1$ SU(2) WZW model can be interpreted in terms of the $S = 1/2$ spinons. Thus the elementary excitation at J'_c is expected to be given by the $S = 1/2$ spinon.

It would also be interesting to explore the higher-spin case. In this case, we can imagine several kinds of intermediate states between the VBS state and the dimer state. For example, in the $S = 2$ case, there exists an intermediate phase: the inhomogeneous VBS state where the number of valence bonds alternates like $1, 3, 1, 3, \ldots$ in a region including the Heisenberg point at least within a variational calculation [71] similar to the one in section 2. The phase transition occurs twice, in agreement with the conjecture by Affleck and Haldane [16]. The above-mentioned RVB picture suggests that the critical theory governing the transitions is also the level-1 SU(2) WZW model, where the $S = 1/2$ spinon is a natural excitation. This speculation is supported by a field-theoretical argument [39]. We do not know what kind of order parameters can distinguish the intermediate phase from the Haldane phase.

Acknowledgments

Two of the authors KT and YN thank Dr Y Nonomura for comments on the numerical calculations. One of the authors (KT) is grateful to Dr S Yamamoto for discussions about the subject.

Appendix A. Calculation of the correlation functions

In this appendix we sketch the calculation of the correlation functions in some detail, mainly to establish the notation. For an account of the basic formulation, see [48].

In general, the presence of the perturbing fields at the fixed point leads to a correction to the scaling behaviour. When the perturbation is irrelevant or marginal, the following formula for the scaling dimension x_i holds [47]:

$$\gamma_i(g) = x_i + 2\pi C_{Vii} g(L) \tag{A1}$$

where C_{Vii} and $g(L)$ denote the coefficient appearing in the operator-product expansion

$$V(z,\bar{z})\phi_i(w,\bar{w}) = \sum_k \frac{C_{Vik}}{(z-w)^{h_V+h_i-h_k}(\bar{z}-\bar{w})^{\bar{h}_V+\bar{h}_i-\bar{h}_k}}\phi_k(w,\bar{w})$$

and the running coupling constant, respectively.

In the following, we are interested in the marginal perturbation

$$V(z,\bar{z}) = \tfrac{2}{\sqrt{3}} J_L(z)\cdot J_R(\bar{z}) \tag{A2}$$

where $\{J_{L/R}\}$ stand for the Kac–Moody currents

$$J_\alpha^+ = :e^{i\sqrt{8}\phi_\alpha}: \qquad J_\alpha^- = :e^{-i\sqrt{8}\phi_\alpha}: \qquad J_\alpha^3 = i\sqrt{2}\partial\phi_\alpha \qquad \alpha = L/R.$$

In order to integrate the renormalization-group equation (RGE), it is necessary to know the long-distance behaviour of $g(L)$. Since V is a marginal perturbation, the β function for $g(L)$ is given by

$$\frac{dg}{d\ln L} = -\pi C_{VVV} g^2 = \tfrac{4}{\sqrt{3}}\pi g^2 \tag{A3}$$

which is integrated to yield [48]

$$g(L) = \frac{g_0}{1 - \frac{4}{\sqrt{3}}\pi g_0 \ln(L/L_0)}. \tag{A4}$$

If the initial coupling constant satisfies $g_0 < 0$, V is a marginally irrelevant perturbation and causes logarithmic corrections to the critical behaviour.

Using the long-distance asymptotics of $g(L)$ (which is obtained by ignoring the term 1 in the denominator of (A4)) and integrating the RGE for two-point functions, we obtain [48]

$$\langle\phi_i(r)\phi_i(0)\rangle \sim \frac{1}{r^{2x_i}}(\ln r)^{\sqrt{3}C_{Vii}}. \tag{A5}$$

If the OPE coefficient C_{Vii} vanishes, the logarithmic correction does not appear.

The coefficients C_{Vii} can be calculated straightforwardly and yield the following results:

$$C_{Vii} = \begin{cases} 0 & \text{for } J^\alpha_{L/R} \quad (x_i = 1) \\ 1/2\sqrt{3} & \text{for } \mathrm{Tr}\, g\sigma \quad (x_i = 1/2) \\ -(\theta/\pi)^2/8\sqrt{3} & \text{for the string operator } (x_i = (\theta/\pi)^2/8). \end{cases} \tag{A6}$$

Putting them into the above formula for two-point functions, we obtain the desired results. The vanishing OPE coefficient C_{Vii} for the Kac–Moody currents implies that the current–current correlator has no logarithmic correction.

References

[1] Haldane F D M 1983 *Phys. Lett.* **93A** 464
[2] Haldane F D M 1983 *Phys. Rev. Lett.* **50** 1153
[3] des Cloizeaux J and Pearson J J 1962 *Phys. Rev.* **128** 2131
[4] Affleck I 1989 *J. Phys.: Condens. Matter* **1** 3047
[5] Botet R, Julien R and Kolb M 1983 *Phys. Rev.* B **28** 3914
[6] Nightingale M P and Blöte H W 1986 *Phys. Rev.* B **33** 659
[7] Buyers W J L, Morra R M, Armstrong R L, Hogan M J, Gerlach P and Hirakawa K 1986 *Phys. Rev. Lett.* **56** 371
[8] Renard J P, Verdaguer M, Regnault L P, Erkelens W A C, Rossat-Mignot J and Stirling W G 1987 *Europhys. Lett.* **3** 945
[9] Katsumata K, Hori H, Takeuchi T, Date M, Yamagishi A and Renard J P 1989 *Phys. Rev. Lett.* **63** 86
[10] Hida K 1992 *Phys. Rev.* B **45** 2207
[11] Kohmoto M and Tasaki H 1992 *Phys. Rev.* **46** 3486
[12] Hida K 1992 *Phys. Rev.* B **46** 8268
[13] Cross M C and Fisher D S 1979 *Phys. Rev.* B **19** 402
[15] Affleck I 1985 *Nucl. Phys.* B **257** [FS14] 397
[16] Affleck I and Haldane F D M 1987 *Phys. Rev.* B **36** 5291
[17] Sutherland B 1975 *Phys. Rev.* B **12** 3795
[18] Uimin G V 1970 *Sov. Phys.–JETP Lett.* **12** 225
[19] Affleck I, Kennedy T, Lieb E and Tasaki H 1988 *Commun. Math. Phys.* **115** 477
[20] Takhtajan L 1982 *Phys. Lett.* **87A** 479
[21] Babujian H M 1982 *Phys. Lett.* **90A** 479
[22] Barber M N and Batchelor M T 1989 *Phys. Rev.* B **40** 4621
[23] Klümper A 1989 *Europhys. Lett.* **9** 815
[24] den Nijs M and Rommelse K 1989 *Phys. Rev.* B **40** 4709
[25] Tasaki H 1991 *Phys. Rev. Lett.* **66** 798
[26] Affleck I and Lieb E 1986 *Lett. Math. Phys.* **12** 57
[27] Fannes M, Nachtergaele B and Werner R F 1992 *Commun. Math. Phys.* **144** 443
[28] Totsuka K and Suzuki M 1995 *J. Phys.: Condens. Matter* **7** 1639
[29] Singh R R P and Gelfand M P 1988 *Phys. Rev. Lett.* **61** 2133
[30] Kato Y and Tanaka A 1994 *J. Phys. Soc. Japan* **63** 1277
[31] Chang K, Affleck I, Hayden G W and Soos Z 1989 *J. Phys.: Condens. Matter* **1** 153
[32] Knabe S 1988 *J. Stat. Phys.* **52** 627
[33] Arovas D P, Auerbach A and Haldane F D M 1988 *Phys. Rev. Lett.* **60** 531
[34] Fáth G and Sólyom J 1993 *J. Phys.: Condens. Matter* **5** 8983
[35] Binder K 1981 *Phys. Rev. Lett.* **47** 693
[36] Binder K 1981 *Z. Phys.* B **43** 119
[37] Hatano N 1994 *J. Phys. A: Math. Gen.* **27** L223
[38] Kennedy T and Tasaki H 1992 *Commun. Math. Phys.* **147** 431
[39] Zamolodchikov A B and Zamolodchikov Al B 1992 *Nucl. Phys.* B **379** 602
[40] Witten E 1984 *Commun. Math. Phys.* **92** 455
[41] Knizhnik V G and Zamolodchikov A B 1984 *Nucl. Phys.* B **247** 83
[42] Affleck I 1989 *Fields, Strings and Critical Phenomena* ed E Brezin and J Zinn-Justin (Amsterdam: Elsevier) ch 10
[43] Goddard P and Olive D 1986 *Int. J. Mod. Phys.* **1** 303
[44] Kadanoff L P and Brown A C 1979 *Ann. Phys.* **121** 318
[45] Yang S-K 1987 *Nucl. Phys.* B **285** 183
[46] Ginsparg P 1989 *Fields, Strings and Critical Phenomena* ed E Brezin and J Zinn-Justin (Amsterdam: Elsevier) ch 1
[47] Cardy J L 1986 *Nucl. Phys.* B **270** [FS16] 186
[48] Affleck I, Gepner D, Schulz H J and Ziman T 1989 *J. Phys. A: Math. Gen.* **22** 511
[49] Ziman T and Schulz H J 1987 *Phys. Rev. Lett.* **59** 140
[50] Blöte H Wm Cardy J L and Nightingale M P 1986 *Phys. Rev. Lett.* **56** 742
[51] Destri C and de Vega H J 1989 *Phys. Lett.* **223B** 365
[52] di Francesco P, Saleur H and Zuber J-B 1987 *Nucl. Phys.* B **285** [FS19] 454
[53] Alcaraz F C and Hatsugai Y 1992 *Phys. Rev.* B **46** 13914
[54] Affleck I 1986 *Nucl. Phys.* B **265** [FS15] 409

[55] Woynarovich F and Eckle H-P 1987 *J. Phys. A: Math. Gen.* **20** L443
[56] Nomura K 1993 *Phys. Rev.* B **48** 16814
[57] Luther A and Peschel I 1975 *Phys. Rev.* **12** 3908
[58] Hida K 1994 *J. Phys. Soc. Japan* **63** 2514
[59] Faddeev L D and Takhtajan L 1984 *J. Sov. Math.* **24** 241
[60] Haldane F D M 1991 *Phys. Rev. Lett.* **66** 1529
[61] Takahashi M 1989 *Phys. Rev. Lett.* **62** 2313
[62] Golinelli O, Jolicoeur Th and Lacaze R 1992 *Phys. Rev.* **45** 9798
[63] White S R and Huse D A 1993 *Phys. Rev.* B **48** 3844
[64] Oshikawa M 1992 *J. Phys.: Condens. Matter* **4** 7469
[65] Hatsugai Y and Kohmoto M 1991 *Phys. Rev.* B **44** 11789
[66] Yamamoto S and Miyashita S 1993 *Phys. Rev.* B **48** 9528
[67] Elstner N and Mikeska H-J 1994 *Phys. Rev.* B **50** 3907
[68] Hida K 1993 *J. Phys. Soc. Japan* **62** 439
[69] Fannes M, Nachtergaele B and Werner R F 1989 *Europhys. Lett.* **10** 633
[70] Takada S 1992 *J. Phys. Soc. Japan* **61** 428
[71] Totsuka K 1994 *unpublished*
[72] Yamamoto S 1995 *Phys. Rev.* B **51** to appear